International Research Journal of Innovations in Engineering and Technology (IRJIET)

ISSN (online): 2581-3048
Volume 9, Issue 11, pp 74-86, November-2025
https://doi.org/10.47001/IRJIET/2025.911009

Effect of Air Inlet Heating on Energy and Exergy Efficiency in Combined Cycle Gas Turbine under Partial Load

[1]*Adha Aditya, [2]Widayat Widayat, [3]Udi Harmoko

[1,2,3]Master Program of Energy, Postgraduate School, Universitas Diponegoro, Semarang 50241, Indonesia
*Corresponding Author's E-mail: adhaadit.ecp@gmail.com

Abstract **- The operational profile of the Indonesian electricity grid often requires Combined Cycle Gas Turbine (CCGT) power plants to operate at partial load, leading to significant thermal efficiency degradation. This study investigates the effect of an integrated air inlet heater, utilizing Low Pressure (LP) Feed Water from the water-steam cycle, to enhance the performance of a GE 09HA.02 CCGT operating at 55% load. A comparative analysis of the plant's operational data was conducted based on energy and exergy principles, with and without the heater activated. The results demonstrate that activating the heater reduced fuel consumption by 7.6 MW and, critically, decreased the plant's total exergy destruction rate from 364.5 MW to 350.9 MW. This improvement was the result of a strategic trade-off: a substantial reduction in the compressor's exergy destruction (by 8.4 MW) outweighed an increase in losses in the Heat Recovery Steam Generator. Consequently, the exergetic efficiency of major components increased, including the compressor (from 92.52% to 95.38%) and the steam turbine (from 90.41% to 91.6%). This work concludes that the integrated air inlet heating strategy is a highly effective method for enhancing the thermodynamic quality and effectiveness of the energy conversion process, offering a validated solution to improve CCGT performance during partial load operation.**

Keywords: Gas Turbine, Air Inlet Heater, Partial Load, Thermal Efficiency, Exergy Analysis.

I. INTRODUCTION

Indonesia's electricity system had a total power generation capacity of 100.69 GW as of the end of 2024, was heavily dominated by fossil fuels, which accounted for approximately 85% of the mix. Coal-fired power plants represented the majority share at 53%, supplemented by combined-cycle gas turbines (27%) and diesel generators (5%). In contrast, the renewable energy sector contributed 14,277 MW (approx. 14.28 GW), with key sources being hydropower (7,270.75 MW), biomass (3,470.67 MW), and geothermal (2,458.95 MW), alongside smaller contributions from solar, wind, and micro-hydro installations [1].

The Indonesian electrical power system is characterized by unique challenges from volatile energy demand. These demand variations lead to fluctuating peak load profiles, which in turn require a generation fleet capable of rapid and dependable response to maintain grid stability. Consequently, the dispatch of power plants at partial load is a frequent operational necessity to balance the network effectively [2]. The technical characteristics of different power plants dictate their roles in maintaining grid stability. Coal-fired steam power plants are fundamentally base load generators; their design prioritizes maximum thermal efficiency during continuous operation and involves lengthy start-up procedures, making them perfect for constant power generation. Combined-cycle gas turbine (CCGT) plants, however, offer the operational flexibility and rapid ramp rates necessary for a load-following function. This allows them to effectively track and respond to variations in electricity demand, thereby stabilizing the grid frequency at its nominal value [3].

The operation of advanced gas turbines at partial load presents a primary engineering challenge concerning efficiency. Despite the excellent responsiveness offered by units like the GE 9HA.02 (up to 88 MW/minute) for grid stabilization, their thermal efficiency is substantially curtailed when running below their optimal design point. Operation at partial load, an off-design condition, leads to a marked decrease in thermal efficiency. This efficiency penalty stems from factors such as an elevated excess air ratio and suboptimal aerodynamics in the turbomachinery blades. Consequently, the plant experiences higher specific fuel consumption and greater emissions per kWh, presenting a core challenge to both economic viability and operational optimization. [4].

Gas turbine performance is highly sensitive to atmospheric conditions, where changes in ambient temperature can significantly influence its power and efficiency [5]. Conventionally, inlet air cooling technologies

International Research Journal of Innovations in Engineering and Technology (IRJIET)
ISSN (online): 2581-3048
Volume 9, Issue 11, pp 74-86, November-2025
https://doi.org/10.47001/IRJIET/2025.911009

are often applied to improve efficiency, particularly in power plants that operate at peak load [6]. However, this approach is less effective for gas turbine units that frequently operate under partial load conditions, a common operating scenario in many power plants, such as in Indonesia. As an innovative solution, a study proposes an inlet air heating technology that utilizes waste heat to raise the air temperature. Contrary to the traditional viewpoint, this method shows considerable potential to improve gas turbine efficiency specifically when operating at partial load. This is because the heating can optimize the operating point of the compressor and turbine, thereby increasing the efficiency of each component [7].

In a study of an 80 MW CCGT plant, Variny & Mierka [8] found that heating the gas turbine inlet air is highly effective for improving efficiency during partial load operation. In contrast to full-load strategies, raising the air temperature boosts HP steam generation in the HRSG, which increases steam turbine output and allows for reduced gas turbine fuel burn. The research quantified savings at 13 m^3/h of natural gas per 1°C of heating. The authors concluded that this method, along with other improvements, could increase the plant's average electrical efficiency from 44% to 45%, showing its significant value for plants that operate frequently below their design capacity.

Zhu et al. [9] introduced a method to improve low-load gas turbine operation by heating the compressor inlet air with its own extraction air. Their findings show a synergistic optimum between inlet temperature and IGV position that boosts stability and efficiency. The study proved that with proper heating, the IGVs could be kept fully open down to 50% load, surpassing the performance of conventional IGV-based control. By enabling components to operate closer to their design specifications, this heating method shows potential to become the primary means of load control, reducing the reliance on IGV modulation.

A significant efficiency improvement for gas turbines at partial load was demonstrated by Liu et al. [7] using a method of inlet air heating with HRSG waste heat. The efficiency gains, attributed to better performance of the compressor and turbine, were maximized by achieving an optimal inlet temperature specific to each load point. At 50% load, for instance, heating the air to an optimal 38°C elevated the gas turbine's efficiency from 26.2% to 31.1%. The study concluded that lower loads benefit from higher heating temperatures, confirming the technology's strong potential for enhancing flexible power generation.

To address partial load inefficiencies in CCGT plants, Yang et al. [10] developed the HEAT method, which involves preheating compressor inlet air with HRSG exhaust gas. The thermodynamic advantage of this approach, particularly with the HEAT-T3-T4 control strategy, stems from achieving a higher compressor discharge temperature. This elevation reduces the exergy destruction that typically occurs in the combustion chamber, leading to enhanced overall cycle performance. The result is a significant increase in combined cycle efficiency by as much as 1.7 percentage points compared to traditional IGV-based load control.

Although the preceding research validates the benefits of inlet air heating, it is consistently limited by the omission of a comprehensive energy and exergy analysis. This oversight means they cannot precisely quantify the thermodynamic shifts in system components or identify the specific sources of reduced exergy destruction that underpin the reported efficiency gains. The current research is designed to fill this analytical void and is distinguished by several novel contributions. First, it investigates the use of Low Pressure Feedwater as the heat source, a thermodynamically unique strategy that leverages an internal steam cycle stream. Second, this study centers on a rigorous energy and exergy analysis to evaluate and refine the performance of this specific heating design. Third, and most essentially, this entire concept is applied to the GE 9HA.02, an advanced H-class gas turbine, to assess the strategy's impact on high-efficiency technology.

This study is conceived to address the critical and persistent challenge of enhancing the operational efficiency of advanced gas turbines, particularly when they are dispatched under the frequently encountered conditions of part-load. Thus, not only contributes to the improvement of the CCGT's global efficiency but also links the research findings to the common operational conditions found in the Indonesian electricity grid. This research is expected to provide new insights into optimizing the operational efficiency of CCGT plants and strengthening their competitiveness in providing a reliable and sustainable electricity supply in Indonesia.

II. METHODOLOGY

2.1 Research Framework

This section outlines the research framework that forms the methodological backbone of this investigation. It has been developed to ensure a logical and systematic workflow for the comprehensive energy and exergy evaluation of the combined-cycle gas turbine plant, targeting improvements in its thermodynamic performance. The framework provides a clear sequence of the research activities and analytical stages involved. A detailed schematic, presented as Figure 1, visually illustrates this entire research process to provide the methodology.

International Research Journal of Innovations in Engineering and Technology (IRJIET)

ISSN (online): 2581-3048

Volume 9, Issue 11, pp 74-86, November-2025

https://doi.org/10.47001/IRJIET/2025.911009

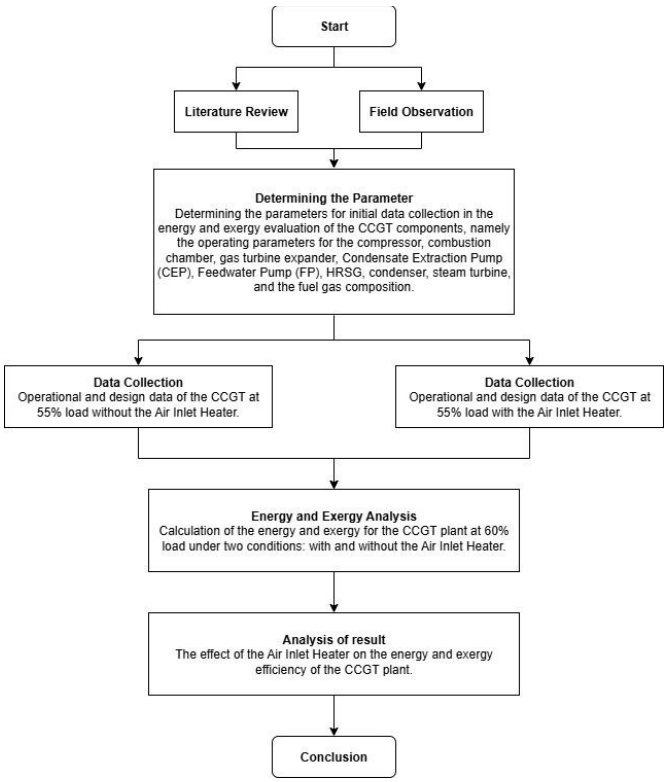

Figure 1: Research Framework

This research methodology commences with a Literature Review and Field Observation to inform the determination of parameters necessary for evaluating the energy and exergy of the CCGT components. Following this, operational data is collected from the plant running at 55% load under two distinct scenarios: first, without the Air Inlet Heater, and second, with the Air Inlet Heater. Both datasets are then utilized to conduct a comparative Energy and Exergy Analysis of the CCGT plant, specifically calculating performance at 60% load under both conditions. Finally, the results are analyzed to determine the precise effect of the Air Inlet Heater on the plant's energy and exergy efficiency, leading to the study's Conclusion.

2.2 System Configuration

The subject of this study is an 880 MW Combined-Cycle Gas Turbine (CCGT) power plant where the CCGT schematic diagram can be seen in Figure 2, a significant contributor to the Indonesian grid capable of meeting the energy demands of five million households. The plant's core configuration is based on a GE 9HA.02 gas turbine and a GE D650 steam turbine, integrated with a heat recovery steam generator (HRSG). This facility represents a top-tier technological solution, characterized by an operational efficiency exceeding 64%, industry-leading low emissions, fuel versatility, and high operational flexibility with a ramp rate of 8 to 12% per minute [11].

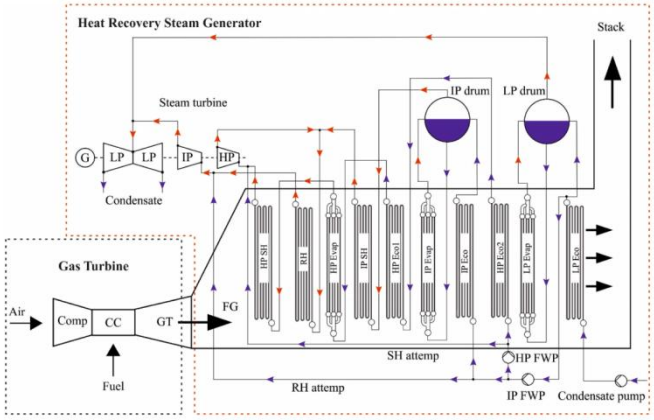

Figure 2: CCGT Schematic Diagram

The steam generation system is a horizontal, triple-pressure HRSG equipped with a reheater and supplementary firing capabilities. Its high-pressure circuit features a once-through evaporator, while the intermediate and low-pressure circuits use natural circulation evaporators. This design, often called a Benson once-through HRSG, is noted for its fast dynamic response. The steam produced drives a three-stage (HP, IP, LP) steam turbine, with a reheat cycle included after the HP stage. The HRSG processes gas turbine exhaust at 638 °C with a flow rate of 1119 kg/s. Figure 1 provides a schematic diagram of the overall combined cycle power plant [12].

2.3 Energy Analysis

Energy analysis, a method rooted in the First Law of Thermodynamics, is a conventional tool for studying energy systems. Its function is to quantify energy interactions by balancing the inputs and outputs of a component or system to uphold the principle of energy conservation (Ivan et al., n.d.). The primary drawback of this method is its purely quantitative nature; it provides no insight into energy quality or the sources of thermodynamic losses [13]. The First Law's premise that all energy is equivalent masks the reality that different energy forms have varying potentials to do work. Therefore, to conduct an energy analysis, one must first apply the foundational mass and energy balance equations to account for all system interactions [14].

$$\sum \dot{m}_i = \sum \dot{m}_e \quad (1)$$

$$\dot{Q} - \dot{W} = \sum \dot{m}_e h_e - \sum \dot{m}_i h_i \quad (2)$$

Where $\dot{Q}$ is the rate of heat transfer, $\dot{W}$ is the work rate, $\dot{m}_i$ and $\dot{m}_e$ denote the mass flow rates entering and exiting the

International Research Journal of Innovations in Engineering and Technology (IRJIET)

ISSN (online): 2581-3048

Volume 9, Issue 11, pp 74-86, November-2025

https://doi.org/10.47001/IRJIET/2025.911009

system, and h_i andh_e represent the specific enthalpy at the inlet and exit, respectively.

1. Gas Turbine

The system functions according to the Brayton cycle, which includes four distinct stages: isentropic compression in a compressor, heat addition at constant pressure within the combustor, isentropic expansion through a turbine, and finally, heat rejection at constant pressure. A thermodynamic analysis can be performed to evaluate the performance and efficiency of each component and the Brayton cycle as a whole using specific equations 3-8.

The compressor work is as follow:

$$\dot{W}_C = \dot{m}_a \ (h_2 - h_1) \tag{3}$$

Where $\dot{m}_a$ denotes the air mass flow rate, and h_2 and h_1 represent the enthalpy of air exiting and entering the compressor, respectively.

The heat input to the combustor is as follows:

$$Q_{in} = \dot{m}_f \text{ x LHV} \tag{4}$$

where $\dot{m}_f$ represents the fuel mass flow rate, and LHV denotes the lower heating value of the fuel.

The gas turbine work is as follows:

$$\dot{W}_{GT} = \dot{m}_{gas} \ (h_3 - h_4) \tag{5}$$

Where $\dot{m}_{gas}$ denotes the air and fuel mass flow rate ($\dot{m}_a + \dot{m}_f$), h_3 and h_4 represent the enthalpy of gas entering and exiting the turbine, respectively.

The heat rejected from the system is as follows:

$$Q_{out} = \dot{m}_{gas} \ (h_4 - h_1) \tag{6}$$

The total Brayton cycle analysis is as follows:

$$\dot{W}_{net} = \dot{W}_{Ta} - \dot{W}_{Ca} \tag{7}$$

$$\eta_{GT} = \frac{\dot{W}_{net}}{Q_{in}} \tag{8}$$

Where $\dot{W}_{net}$ denotes the total cycle work, and η_{GT} represents the cycle thermal efficiency.

2. HRSG

The energy transfer within the HRSG can be understood as a heat exchange process where the heat lost by the hot exhaust gas is gained by the feedwater. The initial energy state is defined by the enthalpy of the hot gas and cool feedwater entering the unit, while the final state is defined by the enthalpy of the cooled gas and the superheated steam exiting it [15].

The energy available in HRSG is as follows:

$$Q_g = \dot{m}_{gas} \ (h_{g.in} - h_{g.out}) \tag{9}$$

$$Q_g = \dot{m}_{gas} c_{p.g} \ (T_{g.in} - T_{g.out}) \tag{10}$$

Where $\dot{m}_{HP}$, $\dot{m}_{IP}$, $\dot{m}_{LP}$ represent feedwater mass flow rate of HP, IP, and LP resepectively, $h_{HP.out}$, $h_{IP.out}$, $h_{LP.out}$ represent entalphy of the superheated steam HP, IP, and LP respectively, $h_{HP.in}$, $h_{IP.in}$, $h_{LP.in}$ represent entalphy of the feedwater HP, IP, and LP respectively.

The energy absorbed by HRSG is as follows:

$$Q_{w/s} = \dot{m}_s \ (h_{s.out} - h_{w.in}) \tag{11}$$

$$\begin{aligned} Q_{w/s} = {} & \dot{m}_{HP} \cdot (h_{HP.out} - h_{HP.in}) \\ & + \dot{m}_{IP} \cdot (h_{IP.out} - h_{IP.in}) \\ & + \dot{m}_{LP} \cdot (h_{LP.out} - h_{LP.in}) \end{aligned} \tag{12}$$

Where $\dot{m}_{HP}$, $\dot{m}_{IP}$, $\dot{m}_{LP}$ represent feedwater mass flow rate of HP, IP, and LP resepectively, $h_{HP.out}$, $h_{IP.out}$, $h_{LP.out}$ represent entalphy of the superheated steam HP, IP, and LP respectively, $h_{HP.in}$, $h_{IP.in}$, $h_{LP.in}$ represent entalphy of the feedwater HP, IP, and LP respectively.

The thermal efficiency of the HRSG is as follows:

$$\eta_{HRSG} = \frac{Q_{w/s}}{Q_g} \tag{13}$$

3. Steam Turbine

The specific shaft work generated by the turbine is equivalent to the specific enthalpy drop of the steam across the unit, from inlet to outlet. [16].

The steam turbine work is as follow:

$$\dot{W}_{ST} = \dot{m}_{steam} \ (h_{s.in} - h_{s.out}) \tag{14}$$

International Research Journal of Innovations in Engineering and Technology (IRJIET)

ISSN (online): 2581-3048

Volume 9, Issue 11, pp 74-86, November-2025

https://doi.org/10.47001/IRJIET/2025.911009

Where $\dot{m}_{steam}$ denotes steam mass flow rate, h_{in} &h_{out} represent entalphy of steam in and out steam turbine, respectively.

4. Feedwater Pump

In the Rankine steam cycle, the feedwater pump's primary function is to pressurize the condensate, moving it from the low-pressure condenser to the high-pressure boiler or HRSG. Although this process requires work, the amount is relatively small compared to the turbine's output because the pump handles liquid water, which is almost incompressible [17].

The feedwater pump work is as follow:

$$\dot{W}_P = \dot{m}_{fw} \ (h_{w.out} - h_{w.in}) \tag{15}$$

Where $\dot{m}_{fw}$ denotes feedwater mass flow rate, $hw_{.in}$& $h_{w.out}$ represent entalphy of water in and out pump, respectively.

5. Condenser

An energy analysis of the condenser equates the heat lost by the condensing steam with the heat gained by the cooling water. This is based on the principle of a direct heat balance, which presumes that the system is adiabatic and all heat is transferred from the steam to the coolant [18].

The condenser's heat rejection rate is as follows:

$$\dot{Q}_{cond} = \dot{m}_{cw} \ c_{p.cw} \ (T_{cw.out} - T_{cw.in}) \tag{16}$$

where $\dot{m}_{cw}$ and $c_{p.cw}$ denotes mass flow rate and specific heat at constant pressure of coolant respectively, $T_{cw.in}$ and $T_{cw.out}$ represent temperature coolant in and exit condenser, respectively.

2.4 Exergy Analysis

Exergy analysis offers a more insightful evaluation of thermodynamic performance than conventional energy analysis because it is built on a non-conservation principle. While energy is always conserved, exergy is destroyed in any real process due to irreversibilities [19]. This loss of exergy, or exergy destruction, represents the actual loss of work potential, making it the true measure of inefficiency [20].This allows an exergy-based approach to accurately identify and quantify the sources of inefficiency within a system, a capability that energy analysis lacks [21]. An exergy analysis is contingent upon first defining the mass and energy balances of a system. From these, and by combining the first and second laws of thermodynamics [14].

The exergy balance equation is obtained as follows:

$$\dot{E}x_Q + \sum \dot{m}_i e_i = \sum \dot{m}_e e_e + \dot{E}x_D + \dot{E}x_W \tag{17}$$

$$\dot{E}x_W = \dot{W} \tag{18}$$

$$\dot{E}x_Q = (1 - \frac{T_0}{T_i}) \ \dot{Q}_{in} \tag{19}$$

Where the subscripts i and e denote the inlet and exit streams of the control volume, respectively, $\dot{E}x_D$ represent exergy destruction rate. Neglecting kinetic and potential exergy, the flow exergy rate is calculated as follows:

$$\dot{E}x = \dot{E}x_{ph} + \dot{E}x_{ch} \tag{20}$$

Where:

$$\dot{E}x = \dot{m} e_x \tag{21}$$

Ignoring kinetic and potential effects, the specific exergy (e_x) of a fluid stream is expressed by the following fundamental equation [22]:

$$e_x = (h - h_0) - T_0 (s - s_0) \tag{22}$$

$$e_x = e_{x.phy} + e_{x.che} \tag{23}$$

$$e_{x.phy} = e_x^T + e_x^P \tag{24}$$

$$e_x^T = c_p \ ((T - T_0) - T_0 \ ln \frac{T}{T_0}) \tag{25}$$

$$e_x^P = R T_0 ln \frac{P}{P_0} \tag{26}$$

The physical exergy is determined using (24), which incorporates temperature and pressure terms calculated from (25) and (26), respectively. In these equations, Where h and s represent specific enthalpy and entropy at the given state respectively, h_0 and s_0 represent specific enthalpy and entropy at the dead state, T_o and P_o represent the temperature and pressure of the surroundings, while c_p is the specific heat of air at constant pressure and R is the gas constant [20].

Chemical exergy exists due to the deviation of a system's chemical makeup (e.g., in the combustion chamber) from that of the environmental dead state [23]. The following equation is used to calculate the resulting exergy flow of the fuel:

$$\xi = \frac{ex_f}{LHV_f} \tag{27}$$

International Research Journal of Innovations in Engineering and Technology (IRJIET)

ISSN (online): 2581-3048

Volume 9, Issue 11, pp 74-86, November-2025

https://doi.org/10.47001/IRJIET/2025.911009

Where ξ is the ratio of the fuel's exergy flow to its LHV. Using the generally accepted value of ξ = 1.06 for natural gas [24], the total fuel exergy can be readily determined.

A detailed, component-level summary of the comprehensive exergy analysis is provided, organized into two distinct tables for clarity. The first, Table 1, systematically lists the calculated rate of exergy destruction for each key component of the power plant, such as the compressor, turbine, and condenser. This data is crucial as it quantifies the magnitude of thermodynamic irreversibilities and identifies the primary locations where work potential is lost. Following this, Table 2 presents the corresponding exergy efficiencies for the same components, offering a normalized metric to evaluate and compare their individual thermodynamic performance.

Table 1: Summary of Exergy Destruction Rate Equations

Plant Components	Exergy Destruction Rate
Air Compressor	$\dot{E}_{D.C} = \dot{W}_C - (\dot{E}x_2 - \dot{E}x_1)$
Combustion Chamber	$\dot{E}_{D.CC} = (\dot{E}x_a + \dot{E}x_f) - \dot{E}x_g$
Gas Turbine	$\dot{E}_{D.GT} = (\dot{E}x_3 - \dot{E}x_4) - \dot{W}_T$
HRSG	$\dot{E}x_{D.HRSG} = (\dot{E}x_{g.in} - \dot{E}x_{g.out}) - (\sum\dot{E}x_{s.out} - \sum\dot{E}x_{w.in})$
Steam Turbine	$\dot{E}x_{D.ST} = (\sum\dot{E}x_{ST.out} - \sum\dot{E}x_{ST.in}) - \dot{W}_{ST}$
Condenser	$\dot{E}x_{D.cond} = (\dot{E}x_{cond.in} - \dot{E}x_{cond.out}) - (\dot{E}x_{cw.out} - \dot{E}x_{cw.in})$
CEP	$\dot{E}x_{D.P} = \dot{W}_P - (\dot{E}x_{out} - \dot{E}x_{in})$
BFP	$\dot{E}x_{D.P} = \dot{W}_P - (\dot{E}x_{out} - \dot{E}x_{in})$

Table 2: Summary of Exergy Efficiency Equations

Plant Components	Exergy Efficiency
Air Compressor	$\epsilon_C = \frac{\dot{E}x_2 - \dot{E}x_1}{\dot{W}_C}$
Combustion Chamber	$\epsilon_{CC} = \frac{\dot{E}x_g}{\dot{E}x_a + \dot{E}x_f}$
Gas Turbine	$\epsilon_T = \frac{\dot{W}_T}{\dot{E}x_3 - \dot{E}x_4}$
HRSG	$\epsilon_{HRSG} = \frac{\sum\dot{E}x_{s.out} - \sum\dot{E}x_{w.in}}{\dot{E}x_{g.in} - \dot{E}x_{g.out}}$
Steam Turbine	$\epsilon_{HRSG} = \frac{\dot{W}_{ST}}{\sum\dot{E}x_{ST.in} - \sum\dot{E}x_{ST.out}}$
Condenser	$\epsilon_{cond} = \frac{\dot{E}x_{cw.out} - \dot{E}x_{cw.in}}{\dot{E}x_{cond.in} - \dot{E}x_{cond.out}}$
CEP	$\epsilon_P = \frac{\dot{E}x_{out} - \dot{E}x_{in}}{\dot{W}_P}$
BFP	$\epsilon_P = \frac{\dot{E}x_{out} - \dot{E}x_{in}}{\dot{W}_P}$

III. RESULTS AND DISCUSSIONS

3.1 Data Collection

The research data are systematically organized to aid in the analysis. The composition of the natural gas fuel is provided as a baseline in Table 3. The plant's operational data are then divided into two main scenarios, corresponding to periods when the Air Inlet Heater/PLE was active and inactive.

International Research Journal of Innovations in Engineering and Technology (IRJIET)
ISSN (online): 2581-3048
Volume 9, Issue 11, pp 74-86, November-2025
https://doi.org/10.47001/IRJIET/2025.911009

Table 3: Fuel Gas Composition

Components	Formula	Volume (%)
Metana	CH4	96,660%
Etana	C2H6	2,300%
Propana	C3H8	0,470%
Butana	C3H8	0,200%
Pentana	C5H12	0,020%
Nitrogen	N2	0,350%
Total		**100,000%**
LHV	kJ/kg	46987

The data for each of these scenarios are presented in detail across several separate tables to simplify the input for calculations. These data include the gas turbine operational data in Table 4, HRSG operational data in Table 5, steam turbine operational data in Table 6, condenser operational data in Table 7, feedwater pump (FWP) operational data in Table 8, and condensate extraction pump (CEP) operational data in Table 9.

Table 4: Gas Turbine Data

Components	Unit	PLE Mode	
		OFF	ON
Air Inlet Press	bar	1,0087	1,00057
Air Inlet Temp	°C	31	31
PLE Inlet Flow	kg/s	-	23,6
PLE Inlet Press	bar	-	19,34
PLE Inlet Temp	°C	-	223,8
PLE Outlet Temp	°C	-	40,3
Inlet Bellmouth Flow	kg/s	648,35	650,28
Inlet Bellmouth Temp	°C	31,487	47,181
CPD	bar	22,065	22,267
CTD	°C	450,27	482,84
Gas Fuel Flow	kg/s	17,592	17,49
Gas Fuel Press	bar	42	42
Gas Fuel Temp before GFPH	°C	7	7
Gas Fuel Temp after GFPH	°C	207,2	207,2
GFPH Water Flow	kg/s	13,2	13,2
GFPH Water Press	bar	50,87	50,87
GFPH Water Temp Inlet	°C	223,8	223,8
GFPH Water Temp Outlet	°C	55,3	55,3
GT Exhaust Flow Outlet	kg/s	727,14	735,34
GT Exhaust Press Outlet	bar	1,03	1,03
GT Exhaust Temp Outlet	°C	676,6	676,87
GT Gross Power	MW	334,6	336,59

International Research Journal of Innovations in Engineering and Technology (IRJIET)
ISSN (online): 2581-3048
Volume 9, Issue 11, pp 74-86, November-2025
https://doi.org/10.47001/IRJIET/2025.911009

Table 5: HRSG Data

PLE Mode	Components	Flow kg/s	Pressure bara	Temperature (°C)
OFF	HRSG gas inlet	727,14	1,03	676,34
	HRSG gas outlet	-	-	77,296
	LP Econ inlet after GFPH return	153,3	23,43	37,5
	LP economizer after preheater	202,7	23,43	50
	Air Inleh Heater (PLE) Supply	-	-	-
	FWP Suction	133,188	19,34	143,8
	FWP Discharge IP	20,56	79,721	144,56
	GFPH Water Inlet	13,2	50,87	223,8
	FWP Discharge HP	112,628	182,96	145,91
	LP Superheater	7,9472	4,0059	244,83
	IP Superheater	7,05	24,842	319,91
	HPT Exhaust/CRH	111,82	22,22	374,2
	RH Superheater	119,05	18,958	584
	HP Superheater	105,85	93,563	588,46
ON	HRSG gas inlet	735,34	1,03	676,7
	HRSG gas outlet	-	-	64,189
	LP Econ inlet after GFPH return	153,3	23,43	37,5
	LP economizer after preheater	202,7	23,43	50
	Air Inleh Heater (PLE) Supply	23,6	19,34	223,8
	FWP Suction	133,22	19,34	143,8
	FWP Discharge IP	20,184	78,386	137,13
	GFPH Water Inlet	13,2	50,87	223,8
	FWP Discharge HP	113,036	181,92	148,97
	LP Superheater	6,908	3,9952	243,13
	IP Superheater	7,0179	24,806	320,66
	HPT Exhaust/CRH	112,22	22,22	374,2
	RH Superheater	119,24	19,336	584,97
	HP Superheater	108,32	95,546	588,66

Table 6: Steam Turbine Data

PLE Mode	Components	Flow (kg/s)	Pressure (bara)	Temperature (°C)
ON	HPT Inlet	105,85	93,498	591,16
	HPT Exhaust	111,82	21,499	372,06
	IPT Inlet	119,05	18,69	588,75
	IPT Exhaust	118,55	3,2133	331,61
	LPT Inlet	7,9472	4,0073	244,7
	LPT Exhaust	125,47	0,07214	37,658
OFF	HPT Inlet	108,32	95,546	591,21
	HPT Exhaust	112,22	21,895	371,63
	IPT Inlet	119,24	19,161	590,41
	IPT Exhaust	118,72	3,2324	331,81
	LPT Inlet	6,9018	3,9993	242,85
	LPT Exhaust	122,13	0,071572	38,189

International Research Journal of Innovations in Engineering and Technology (IRJIET)
ISSN (online): 2581-3048
Volume 9, Issue 11, pp 74-86, November-2025
https://doi.org/10.47001/IRJIET/2025.911009

Table 7: Condenser Data

Components	Unit	PLE Mode	
		OFF	ON
Cond press	mbara	55,689	56,912
Cond temp	C	39,058	39,415
Cond duty	GJ/h	1099,9	1084
Cond effectiveness	%	52,62	56,074
ST LP exhaust flow	kg/s	127,56	126,71
ST exhaust temp	C	39,058	39,415
ST exhaust enthalpy	kJ/kg	2552,6	2535,3
Condensate flow	kg/s	127,81	126,96
CW flow	kg/s	18319	17853
CW inlet temp	C	31,055	31,821
CW outlet temp	C	35,267	36,079

Table 8: BFP Data

Components	Unit	PLE Mode			
		OFF		ON	
		FWP-1	FWP-2	FWP-1	FWP-2
Inlet press	bara	34,299	34,171	32,723	32,586
Inlet temp	C	144,94	144,94	135,87	135,87
Inlet flow	kg/s	66,594	66,594	66,61	66,61
HP outlet press	bara	183,01	182,91	181,95	181,89
HP outlet temp	C	145,73	145,73	139,46	139,46
HP outlet flow	kg/s	56,314	56,314	56,518	56,518
IP outlet press	bara	79,721	79,721	78,386	78,386
IP outlet temp	C	144,56	144,56	137,13	137,34
IP outlet flow	kg/s	10,28	10,28	10,092	10,092
Motor power	MW	1,7871	1,8329	1,8138	1,8252
Efficiency	%	54,062	52,739	53,136	52,838
Head	meters	1641,1	1641,5	1632,8	1633,6
Shaft power	MW	1,7871	1,8329	1,8138	1,8252
NPSH	meters	333,05	333,05	323,21	323,21

Table 9: CEP Data

Components	Unit	PLE Mode			
		OFF		ON	
		CEP-1	CEP-2	CEP-1	CEP-2
Inlet press	bara	0,417	0,417	0,417	0,417
Inlet temp	C	34,825	34,825	35,218	35,218
Inlet flow	kg/s	68,338	68,338	85,747	85,747
Outlet press	bara	36,859	36,859	36,419	36,419
Outlet temp	C	27,901	27,901	32,602	32,602
Outlet flow	kg/s	63,338	68,338	85,747	85,747
Motor power	MW	0,45955	0,47426	0,49315	0,51511
Efficiency	%	58,539	56,725	67,62	64,728
Head	meters	373,79	373,79	369,33	369,33
Shaft power	MW	0,42795	0,44164	0,4593	0,47982
NPSH	meters	3,7061	3,7061	3,6941	3,6941

International Research Journal of Innovations in Engineering and Technology (IRJIET)

ISSN (online): 2581-3048

Volume 9, Issue 11, pp 74-86, November-2025

https://doi.org/10.47001/IRJIET/2025.911009

3.2 Energy Analysis

The mathematical models of the CCGT, which were derived from energy and exergy principles in the previous section, were applied to a practical case study using operational data from unit GE 09HA.02. Table 3-9 presents the data collection, which specifies operational data during PLE active and inactive for the main components of the topping (gas) and bottoming (steam) cycles. Based on this data, the thermodynamic properties and thermal efficiency of the power cycle were determined.

Table 10: Result of Energy Analysis during PLE Inactive

Components		Value (MW)	Efficiency (%)
Compressor Work	$\dot{W}_C$	316,723	-
CC Heat Input	Q_{in}	866,939	-
GT Work	$\dot{W}_{GT}$	648,3	38,25
CEP	$\dot{W}_{CEP}$	0,87	-
FWP	$\dot{W}_{FWP}$	3,572	-
HRSG	$Q_{w/s}$	416,404	85,87
	Q_g	484,944	
ST Work	$\dot{W}_{ST}$	188,641	97,1
Condenser Heat Reject	Q_{cond}	305,552	-

The activation of the air intake heater initiates a sequential and interconnected series of thermodynamic effects, beginning with a fundamental alteration of the topping gas turbine cycle's performance profile. The first and most direct consequence of heating the inlet air is the increased work required by the compressor due to the reduction in air density [25]. A quantitative analysis shows that the compressor's power consumption significantly increases from 316,723 MW with the PLE inactive in Table 10 to 330,191 MW with the PLE active in Table 11, representing an additional parasitic load of 13,468 MW. However, this increased load is a strategic thermodynamic investment, as it yields substantial savings in the combustion chamber. With the compressed air entering at a higher initial enthalpy, less fuel is required to reach the target turbine inlet temperature. This is evidenced by the reduction in the required CC Heat Input from 866,939 MW to 859,386 MW, a net fuel energy saving of 7,553 MW. The synergistic effect of this fuel saving ultimately results in a more powerful expansion phase, increasing the Gas Turbine (GT) work output from 648,3 MW to 665,6 MW. This overall performance enhancement confirms that the benefits of more efficient combustion outweigh the cost of higher compression work, which is reflected in the gas turbine's efficiency increasing from 38,25% to 39,03%.

Table 11: Result of Energy Analysis during PLE Active

Components		Value (MW)	Efficiency (%)
Compressor Work	$\dot{W}_C$	330,191	-
CC Heat Input	Q_{in}	859,386	-
GT Work	$\dot{W}_{GT}$	665,6	39.03
CEP	$\dot{W}_{CEP}$	0,94	-
FWP	$\dot{W}_{FWP}$	3,6	-
HRSG	$Q_{w/s}$	439,392	87,68
	Q_g	501,13	
ST Work	$\dot{W}_{ST}$	191,289	97,09
Condenser Heat Reject	Q_{cond}	301,032	-

The cascading effects of this optimized topping cycle then propagate positively to the bottoming steam cycle, with the most significant impact observed in the performance of the HRSG. The higher-energy exhaust gas from the more efficient gas turbine serves as a superior heat source for steam generation. As a result, the heat absorbed by the water/steam cycle within the HRSG substantially increases from 416,404 MW to 439,392 MW, an additional energy recovery of 22,988 MW. This not only increases the quantity of recovered heat but also enhances the heat transfer effectiveness of the HRSG itself, with its efficiency rising from 85,87% to 87,68%. This more intensive steam generation process directly yields a higher ST work output, which increases from 188,641 MW to 191,289 MW. In conclusion, the combination of all these improvements results in a more productive and efficient power plant overall. The system not only produces a greater net power output increasing from 515,78 MW to 522,16 MW, but also rejects less heat to the environment, as evidenced by the decrease in Condenser Heat Rejection from 305,552 MW to 301,032 MW. This provides conclusive evidence that the implementation of the air intake heater is a holistically beneficial strategy for improving the plant's global thermodynamic performance and energy conversion efficiency.

3.3 Exergy Analysis

An exergy analysis of each main component of the combined-cycle gas turbine (CCGT) power plant provides crucial insights into the location and magnitude of true thermodynamic inefficiencies, which cannot be revealed by energy analysis alone. Component-level exergy analysis provides a quantitative map of the sources of thermodynamic inefficiency within the CCGT system illustrated through graphs in Figure 3-4. The results consistently identify the combustion chamber (CC) as the primary center of irreversibility, regardless of its operational mode. This

International Research Journal of Innovations in Engineering and Technology (IRJIET)
ISSN (online): 2581-3048
Volume 9, Issue 11, pp 74-86, November-2025
https://doi.org/10.47001/IRJIET/2025.911009

component alone is responsible for over two-thirds (approximately 68%) of the total work potential lost throughout the plant, with exergy destruction values of 240,942 MW in the inactive state and 246,952 MW in the active state. Second in this hierarchy of inefficiency is the Heat Recovery Steam Generator (HRSG), which is also a significant source of losses. Below it, turbomachinery components such as the compressor, gas turbine, and steam turbine each contribute a smaller fraction of the total destruction, while the irreversibilities in the condenser and feedwater pump system are comparatively negligible. This hierarchy of losses confirms that the greatest opportunities for thermodynamic efficiency improvements lie in mitigating the irreversibilities within the combustion and heat transfer processes.

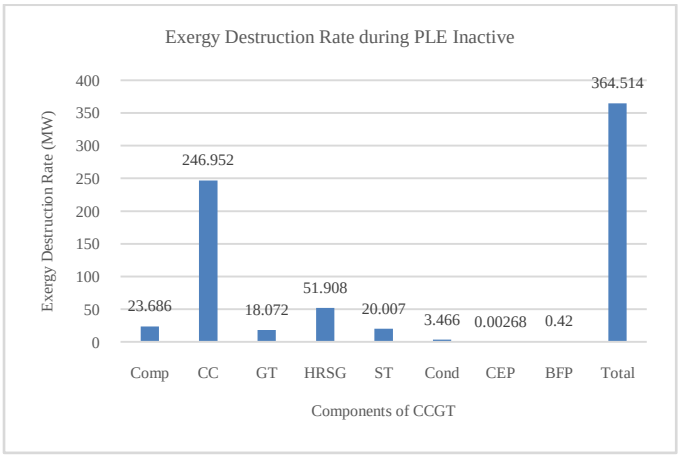

Figure 3: Exergy Destruction Rate during PLE Inactive

The activation of the air intake heater (PLE) effectively re-engineers the distribution of thermodynamic losses within the plant, resulting in a strategic trade-off. The most significant improvement occurs in the compression process, which becomes substantially more reversible, as evidenced by the compressor's exergy destruction decreasing sharply from 23.686 MW to 15.25 MW. This gain is achieved at the cost of higher irreversibilities in the heat recovery process, as this strategy simultaneously increases the exergy destruction in the HRSG from 51.908 MW to 57.545 MW. However, the substantial reduction in compressor losses far outweighs the increase in HRSG losses. This leads to a net overall improvement in the plant's thermodynamic performance, confirmed by the total exergy destruction rate decreasing from 364.514 MW to 350.892 MW when the PLE is active.

The analysis of exergy efficiency with the PLE inactive provides a baseline for performance evaluation. This data in Figure 5 indicates that components such as the CEP and the Gas Turbine operate at high efficiencies of 99,69% and 97,29%, respectively. In contrast, the lowest exergy efficiencies are identified in the Combustion Chamber (CC) at 79,33% and the Condenser at 38,29%, marking them as the primary sources of thermodynamic imperfection. When the PLE is activated, an increase in exergy efficiency is observed across nearly all components. This systemic increase suggests an improvement in the quality of the energy conversion processes throughout the plant.

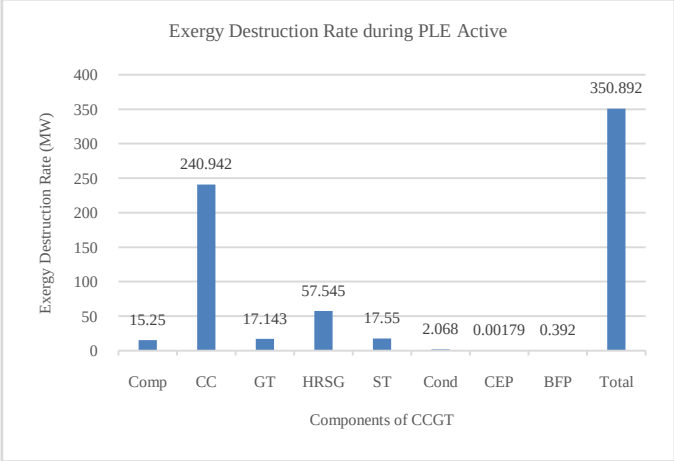

Figure 4: Exergy Destruction Rate during PLE Active

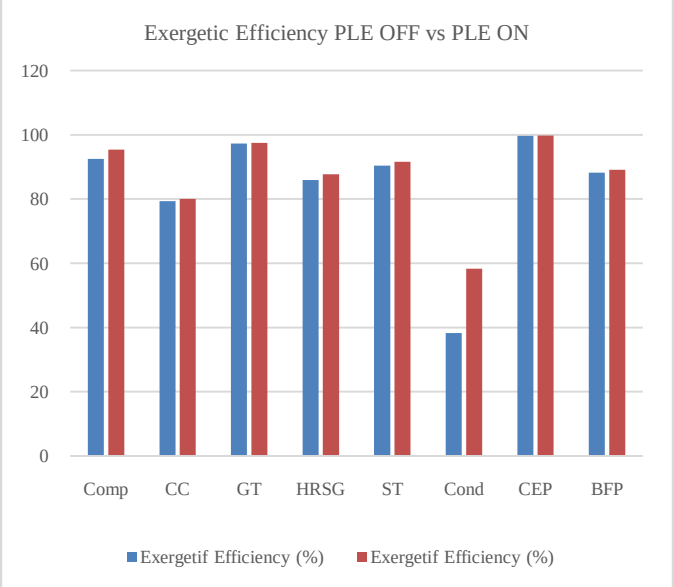

Figure 5: Exergy Efficiency PLE OFF vs PLE ON

The most significant efficiency changes are observed in key components. The exergy efficiency of the HRSG increases from 85,87% to 87,68%, a result consistent with the reduced exergy destruction rate previously calculated for its heat transfer process. The largest numerical increase occurs in the Condenser, where efficiency rises from 38,29% to 58,26%, reflecting the lower heat rejection load. Furthermore, the Combustion Chamber's efficiency improves from 79.33% to 80,06%. A notable finding pertains to the Compressor, where exergy efficiency increases from 92,52% to 95,38%. This occurs despite an increase in its absolute exergy destruction,

ISSN (online): 2581-3048
Volume 9, Issue 11, pp 74-86, November-2025
https://doi.org/10.47001/IRJIET/2025.911009

which suggests a more effective compression process relative to the work consumed. Collectively, these results confirm that the PLE strategy is effective in enhancing the thermodynamic performance of individual components as well as the energetic integration of the overall system.

IV. CONCLUSION

This research was conducted to address the operational challenge faced by Combined Cycle Gas Turbine (CCGT) plants in the Indonesian electricity grid, where frequent dispatch at partial load leads to significant thermal efficiency degradation. To overcome this issue, this study evaluated the implementation of an integrated air inlet heater, which utilizes Low Pressure (LP) Feed Water from the steam cycle to preheat the compressor's intake air on a GE 09HA.02 gas turbine operating at 55% load. The comparative energy analysis of operational data yielded conclusive results, although compressor work increased, compressor's exergy destruction decrease, showing a fuel consumption decreased by 7.553 MW, leading to a higher net power output and less heat rejection. These energy gains were achieved through a series of component-level performance enhancements across the entire plant.

A key finding is that activating the air inlet heater leads to a significant net reduction in the plant's total exergy destruction rate, which decreased from 364.5 MW to 350.9 MW. This overall improvement in thermodynamic perfection is the result of a strategic trade-off. The most substantial gain was a sharp decrease in the compressor's exergy destruction from 23.7 MW to 15.3 MW, indicating a more reversible and efficient compression process. This significant improvement in the compressor was achieved at the cost of higher irreversibilities in the heat recovery process. While the exergy destruction in the HRSG increased from 51.908 MW to 57.545 MW, its exergy efficiency also paradoxically rose from 85.87% to 87.68%. This indicates that although the total work potential lost in the HRSG was higher due to a greater energy throughput, the process became more effective at its primary function of transferring useful exergy from the hot exhaust gas to the steam cycle. In conclusion, the study provides data-driven evidence that the air inlet heater is a holistically beneficial strategy that enhances overall plant efficiency by fundamentally improving the compression process.

REFERENCES

[1] E. Listiani Dewi, "Laporan Kinerja Ditjen EBTKE Tahun 2024," 2025.

[2] A. Liebman -Monash *et al.*, "A Roadmap for Indonesia's Power Sector: How Renewable Energy Can Power Java-Bali and Sumatra Study Team: A Roadmap for Indonesia's Power Sector: How Renewable Energy Can Power Java-Bali and Sumatra," 2019. [Online]. Available: www.agora-energiewende.org|info@agora-energiewende.de

[3] H. H. Coban and W. Lewicki, "Flexibility in Power Systems of Integrating Variable Renewable Energy Sources," *Journal of Advanced Research in Natural and Applied Sciences*, vol. 9, no. 1, pp. 190–204, Mar. 2023, doi: 10.28979/jarnas.1137363.

[4] M. Moliere, J. N. Jaubert, R. Privat, and T. Schuhler, "Stationary gas turbines: An exergetic approach to part load operation," *Oil and Gas Science and Technology*, vol. 75, 2020, doi: 10.2516/ogst/2020001.

[5] F. Basrawi, T. Yamada, K. Nakanishi, and S. Naing, "Effect of ambient temperature on the performance of micro gas turbine with cogeneration system in cold region," *Appl Therm Eng*, vol. 31, no. 6–7, pp. 1058–1067, May 2011, doi: 10.1016/j.applthermaleng.2010.10.033.

[6] M. Saghafifar and M. Gadalla, "Innovative inlet air cooling technology for gas turbine power plants using integrated solid desiccant and Maisotsenko cooler," *Energy*, vol. 87, pp. 663–677, Jul. 2015, doi: 10.1016/j.energy.2015.05.035.

[7] Z. T. Liu *et al.*, "Effect of inlet air heating on gas turbine efficiency under partial load," *Energies (Basel)*, vol. 12, no. 17, Aug. 2019, doi: 10.3390/en12173327.

[8] M. Variny and O. Mierka, "Improvement of part load efficiency of a combined cycle power plant provisioning ancillary services," *Appl Energy*, vol. 86, no. 6, pp. 888–894, 2009, doi: 10.1016/j.apenergy.2008.11.004.

[9] W. Zhu *et al.*, "Improvement of part-load performance of gas turbine by adjusting compressor inlet air temperature and IGV opening," *Frontiers in Energy 2021*, pp. 1–17, May 2021, doi: 10.1007/S11708-021-0746-Z.

[10] Y. Yang, Z. Bai, G. Zhang, Y. Li, Z. Wang, and G. Yu, "Design/off-design performance simulation and discussion for the gas turbine combined cycle with inlet air heating," *Energy*, vol. 178, pp. 386–399, Jul. 2019, doi: 10.1016/j.energy.2019.04.136.

[11] F. Alobaid, J. Wieck, and B. Epple, "Dynamic process simulation of a 780 MW combined cycle power plant during shutdown procedure," *Appl Therm Eng*, vol. 236, Jan. 2024, doi: 10.1016/j.applthermaleng.2023.121852.

[12] GE Gas Power, "Manual Book: Combined Cycle Operation Jawa-1," 2021. [Online]. Available: http://sc.ge.com/*pstraintemp

[13] I. Dincer and Y. A. Cengel, "Energy, Entropy and Exergy Concepts and Their Roles in Thermal Engineering," 2001. [Online]. Available:

ISSN (online): 2581-3048
Volume 9, Issue 11, pp 74-86, November-2025
https://doi.org/10.47001/IRJIET/2025.911009

www.mdpi.org/entropy/http://www.geocities.com/ibrahimdincer

[14] M. Ameri and N. Enadi, "Journal of Power Technologies 92 (3) (2012) 183-191 Thermodynamic modeling and second law based performance analysis of a gas turbine power plant (exergy and exergoeconomic analysis)."

[15] A. Temraz, A. Rashad, A. Elweteedy, F. Alobaid, and B. Epple, "Energy and exergy analyses of an existing solar-assisted combined cycle power plant," *Applied Sciences (Switzerland)*, vol. 10, no. 14, Jul. 2020, doi: 10.3390/app10144980.

[16] Y. Wang and P. Wang, "Application of stable flow energy equation in steam turbine and other power machines," in *IOP Conference Series: Earth and Environmental Science*, Institute of Physics Publishing, May 2020. doi: 10.1088/1755-1315/474/5/052087.

[17] K. Madan and O. K. Singh, "Second Law-Based Assessment of Combined Cycle Power Plant," *Evergreen*, vol. 10, no. 1, pp. 356–365, Mar. 2023, doi: 10.5109/6781093.

[18] A. H. Qurrahman, W. Wilopo, S. P. Susanto, and M. Petrus, "Energy and Exergy Analysis of Dieng Geothermal Power Plant," *International Journal of Technology*, vol. 12, no. 1, pp. 175–185, 2021, doi: 10.14716/ijtech.v12i1.4218.

[19] F. Indriyati, C. P. Mahandari, and M. Yamin, "Advanced Exergy Analysis on the Turbofan Engine," *Journal of Novel Engineering Science and Technology*, vol. 3, no. 03, pp. 79–85, Jun. 2024, doi: 10.56741/jnest.v3i03.543.

[20] T. K. Ibrahim *et al.*, "Thermal performance of gas turbine power plant based on exergy analysis," *Appl Therm Eng*, vol. 115, pp. 977–985, 2017, doi: 10.1016/j.applthermaleng.2017.01.032.

[21] Q. Younus Hamid, A. Ahmed, A. Muhyuddin Hassan, A. Hasan Ahmed, A. Mahmoud Ahmed, and Q. Younis Hamid, "Exergy and Energy Analysis of 150 MW Gas Turbine Unit: A Case Study," *Journal of Advanced Research in Fluid Mechanics and Thermal Sciences Journal homepage*, vol. 67, pp. 186–192, 2020, [Online]. Available: www.akademiabaru.com/arfmts.html

[22] A. Haouam, C. Derbal, and H. Mzad, "Thermal performance of a gas turbine based on an exergy analysis," in *E3S Web of Conferences*, EDP Sciences, Nov. 2019. doi: 10.1051/e3sconf/201912801027.

[23] F. A. Hatem, M. K. A. Alhumairi, M. A. Al-Obaidi, A. T. Mohammad, and A. S. K. Darwish, "Upgrading gas turbine efficiency for sustainable power generation: An energy and exergy analyses," *Results in Engineering*, vol. 26, Jun. 2025, doi: 10.1016/j.rineng.2025.105489.

[24] A. Harutyunyan, K. Badyda, and Ł. Szablowski, "Energy and exergy analysis of complex gas turbines systems powered by a mixture of hydrogen and methane," *Int J Hydrogen Energy*, vol. 144, pp. 713–725, Jul. 2025, doi: 10.1016/j.ijhydene.2025.02.378.

[25] A. De Sa and S. Al Zubaidy, "Gas turbine performance at varying ambient temperature," *Appl Therm Eng*, vol. 31, no. 14–15, pp. 2735–2739, 2011, doi: 10.1016/j.applthermaleng.2011.04.045.

Citation of this Article:

Adha Aditya, Widayat Widayat, & Udi Harmoko. (2025). Effect of Air Inlet Heating on Energy and Exergy Efficiency in Combined Cycle Gas Turbine under Partial Load. *International Research Journal of Innovations in Engineering and Technology - IRJIET*, 9(11), 74-86. Article DOI https://doi.org/10.47001/IRJIET/2025.911009

****

